Supporting information for:

Nanoplastics decrease the toxicity of a complex PAH mixture but impair mitochondrial energy production in developing zebrafish

Rafael Trevisan[1,*], Ciara Voy[1], Shuxin Chen[2], Richard Di Giulio[1].

[1]Nicholas School of the Environment, Duke University, Durham, NC 27708, USA.
[1]North Carolina School of Science and Mathematics, Durham, NC 27705, USA.

* Corresponding author: rafael.trevisan@duke.edu

Table of contents

Table S1

Table S1: Concentration (ng/mL, average ± SD) of 36 PAHs in the Elizabeth River Sediment Extract (n =5). Original data published elsewhere [15].

	Concentration (ng/mL)
Naphthalene	1694.0 ± 104.8
Phenanthrene	671.6 ± 29.1
Fluoranthene	437.1 ± 28.7
Acenaphthene	329.4 ± 47.1
Carbazole	300.4 ± 60
Pyrene	288.7 ± 21.3
Fluorene	242.6 ± 20.3
Dibenzofuran	178.6 ± 9.7
1-methylnaphthalene	152.5 ± 17.3
Anthracene	87.6 ± 3.3
1,2-Benzanthracene	84.1 ± 6.3
Benzo(b)fluoranthene	69.2 ± 3.2
Chrysene	61.8 ± 4.3
3,4-benzofluorene	48.3 ± 5.9
2-methylphenanthrene	47.2 ± 4.4
1,2-benzofluorene	46.5 ± 4.7
Dibenzothiophene	46.4 ± 1.9
Benzo(a)pyrene	40.2 ± 3.1
2,6-dimethylnaphthalene	27.3 ± 5.3
Benzo(e)pyrene	28.4 ± 1.6
Benzo(k)fluoranthene	26.5 ± 2.2
1-methylphenanthrene	20.6 ± 2.6
Indeno(1,2,3-c,d)pyrene	15.9 ± 3.6
Benzo(g,h,i)perylene	15.6 ± 3.8

Acenaphthylene	13.1 ± 3.4
Benzo(c)phenanthrene	13.6 ± 1.5
Perylene	8.6 ± 0.5
(Table S1 Continued)	
Retene	4.6 ± 3.2
Benzo(a)fluoranthene	7.2 ± 0.6
Dibenzo(a,l)pyrene	5.7 ± 0.8
Benzo(b)chrysene	4.0 ± 0.5
Picene	3.6 ± 0.4
Dibenzo(a,j)anthracene	2.9 ± 0.4
Dibenzo(a,h)anthracene	0.4 ± 0.2
3-methylcholanthrene	0.3 ± 0.0
Total measured PAHs	5073 ± 409

Material and methods: oxygen consumption rates

For embryonic assays, each experiment consisted of 2 petri dishes, while for larval assays each experiment consisted of 1 petri dish. Animals were assayed at 24 hpf (embryos) or 96 hpf (larvae).

The *in vivo* OCR was assessed in 24 hpf embryos using the XFe24 Extracellular Flux Analyzer (Agilent Instruments, Santa Clara, CA, USA) according to a previously established protocol (Stackley et al., 2011). For this assessment, embryos were staged as two embryos per well in a 24-well plate with 700 µL of .065 ‰ ASW and a capture screen was carefully loaded on top. A total of 5-6 wells were used per group per experiment, with additional 2 wells as blanks (no embryos). Each measurement cycle consisted of 2 min intervals of mixing, waiting, and measurement periods. Basal OCR was measured over 8 cycles, prior to the injection of pharmacological agents: i) the mitochondrial uncoupler carbonyl cyanide 4-(trifluoromethoxy) phyenylhydrazone (FCCP) (2.5 µM; for maximal OCR), ii) the cytochrome c oxidase inhibitor sodium azide (NaN_3) (6.25 mM; for non-mitochondrial OCR), or iii) the ATP synthase inhibitor oligomycin A (9.4 µM; for OCR due to proton leak). As shown in the figure below (Fig. S1), these OCR values were also used to calculate mitochondrial basal respiration (basal - NaN_3), maximal mitochondrial respiration (FCCP - NaN_3), mitochondrial spare capacity (FCCP - basal), and ATP-linked respiration (basal - oligomycin A). By calculating how much the ATP-link OCR represents to the mitochondrial basal OCR, mitochondrial coupling efficiency is estimated (%). The internal temperature of the XF^{e}24 Extracellular Flux Analyzer remained between 28–28.5°C for the duration of all assays. The experiments were repeated 4 times (n = 20 - 24).

The *in vivo* OCR was also assessed in 96 hpf as described above, with minor modifications based on a previously study published [18]. One larva was staged per well with 450 µL of .065 ‰ ASW and the addition of a capture screen. Before basal OCR was measured, 125 mg/ml tricaine was added to each well to prevent larval movement and unstable respiration; OCR measurements started 12 min after tricaine addition. All OCR measurements were carried out as described above, except that oligomycin A was not used as larvae appeared to not be responsive to this chemical. The experiment was repeated 3 times (n = 15 - 18).

Figure S1

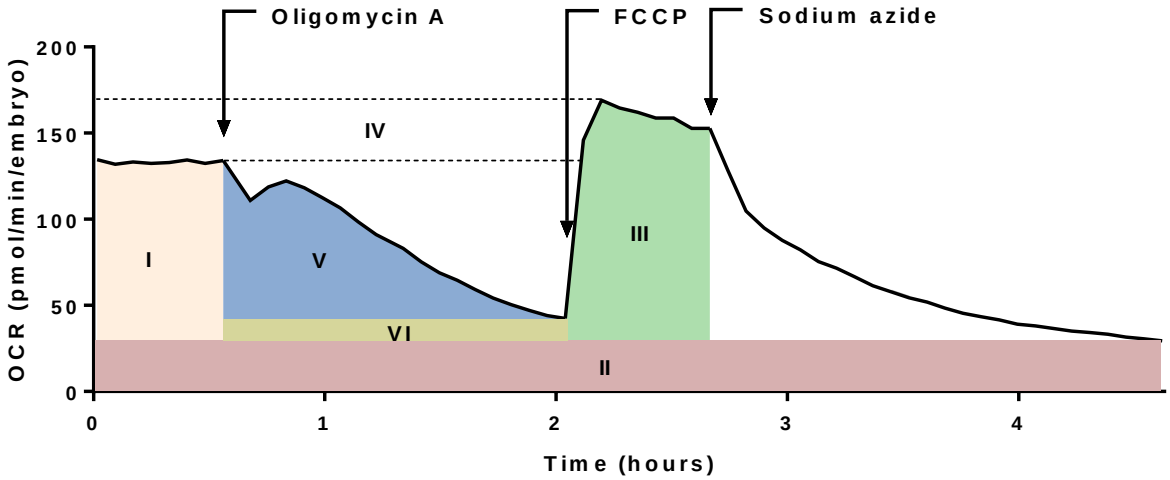

Figure S1: different *in vivo* oxygen consumption rates (OCR) determined in zebrafish embryos or larvae. The basal respiration was called total basal OCR (I + II) and is comprised of a mitochondrial (I) and non-mitochondrial fraction (II, achieved by the use of sodium azide); the maximal embryonic OCR (total maximal, II + III) is induced by the use of the ionophore FCCP and is the sum of the non-mitochondrial fraction (II) and the mitochondrial maximal OCR (III); the difference between the total maximal and total basal is the mitochondrial spare capacity (IV); and by using the ATP synthase inhibitor oligomycin A it is possible to divide the mitochondrial basal OCR into ATP-linked (V) and proton leak (VI) fractions. In addition to these parameters, the mitochondrial coupling efficiency is also calculated to estimate how much of the mitochondrial basal OCR is related to ATP synthesis.

Figure S2

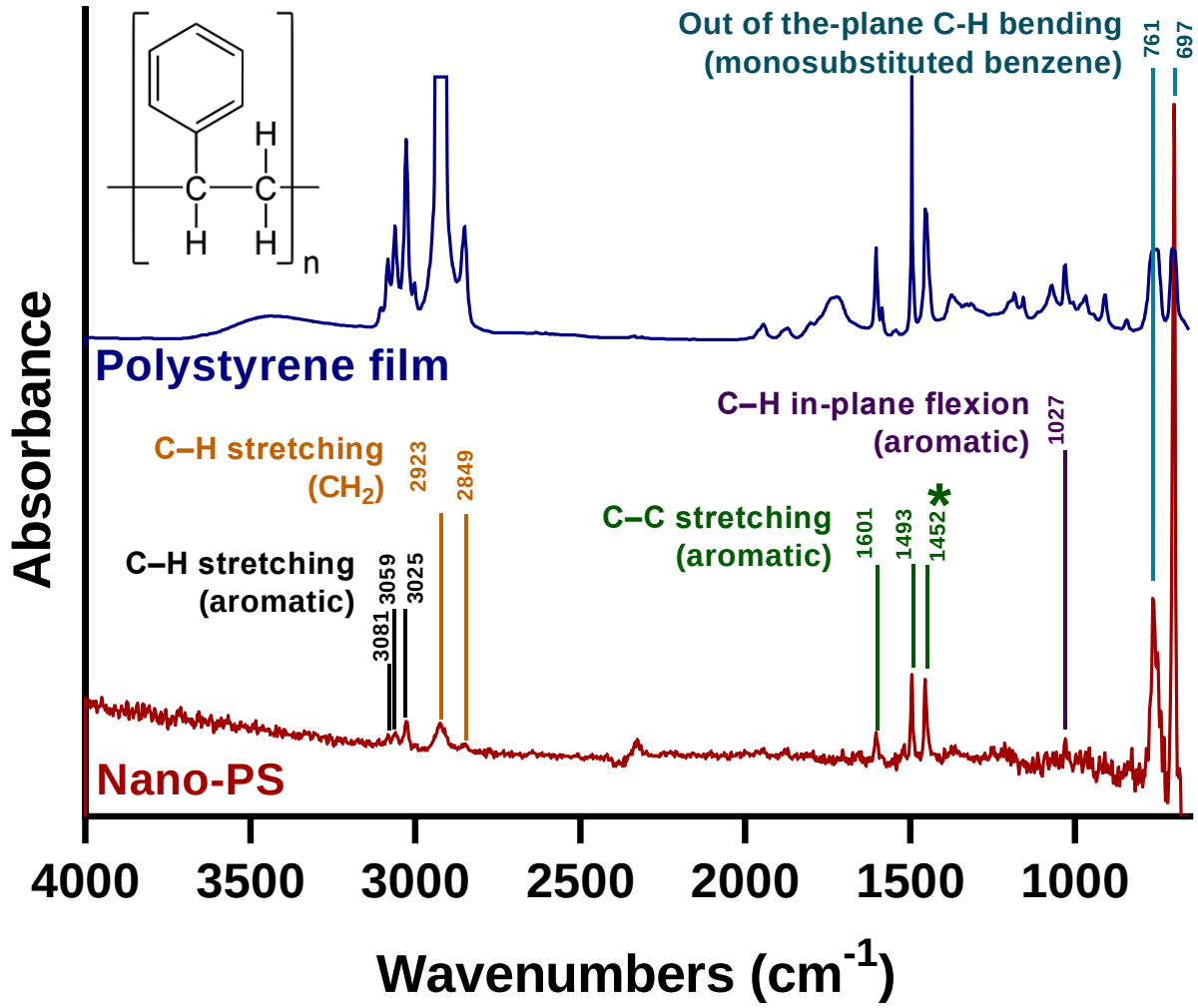

Figure S2: FT-IR spectrum of 50 nm polystyrene nanoparticles (Nano-PS, red line) and a reference polystyrene film (blue line) collected by ATR-FTIR spectroscopy. Bands positively identified in the Nano-PS spectrum are indicated in different colors, which corresponds to their functional groups. Nano-PS particles were filtered to remove interfering agents (sodium dodecyl sulfate and sodium azide) and air-dried prior the analysis. * The band at 1452 cm^{-1} may also result from the deformation vibration of CH_2 + C=C of the aromatic ring.

Figure S3

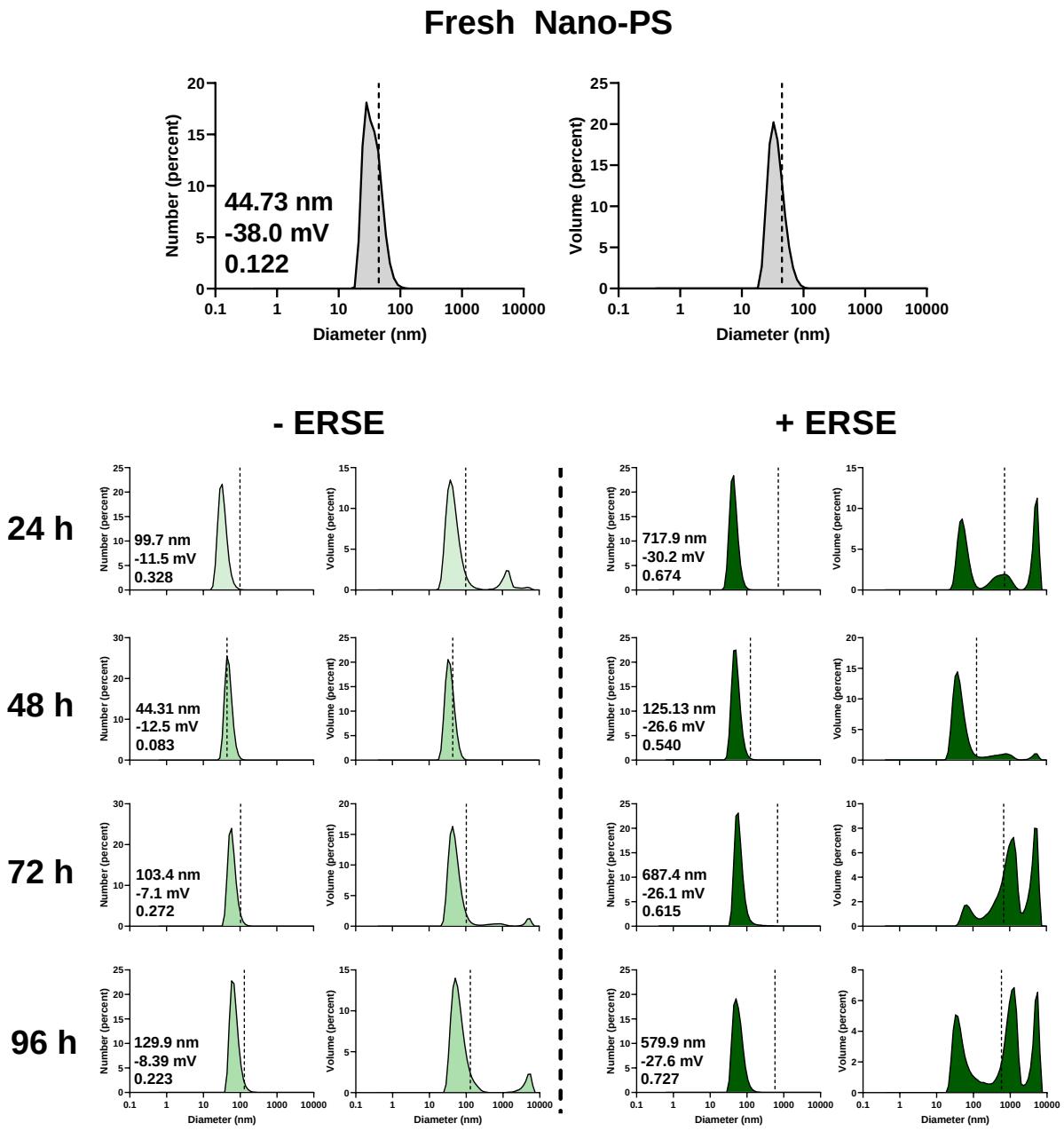

Figure S3: Dynamic light scattering and zeta potential analysis of 44 nm polystyrene nanoparticles (Nano-PS, 10 ppm). Top panel: analysis of freshly prepared Nano-PS (in 30% Danieau). Bottom panel: analysis of Nano-PS after 24, 48, 72, or 96 hours of incubation in 30 % Danieau at 28 ˚C and 60 rpm under 14:10 hours light/dark cycle, in the presence (+ ERSE, dark

green) or not (- ERSE, light green) of a real-world environmental mixture of PAHs (Elizabeth River Sediment Extract – ERSE, 5%). Results for each time point are presented as the distribution of particle sizes according to the intensity (left graph) and volume/mass (right graph). The dashed line indicates the average particle size, which is also shown in nm together with the zeta potential (in mV) and the polydispersity index (ranging from 0 to 1). Samples were diluted 10 times in 30% Danieau prior analysis.

Figure S4

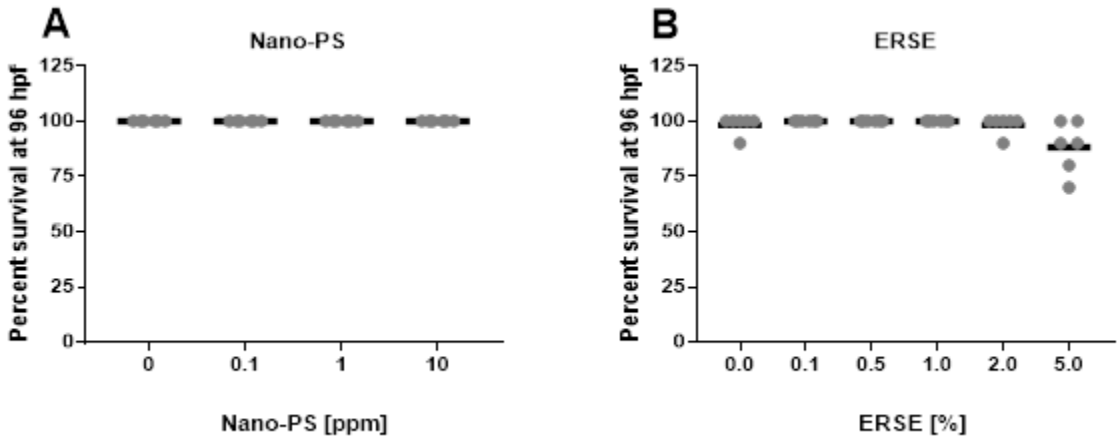

Figure S4: Survival rates of zebrafish larvae exposed to 44 nm nanopolystyrene particles (Nano-PS, A) or a real world environmental PAH mixture (Elizabeth River Sediment Extract – ERSE, B). Animals were exposed at 6 hours post fertilization (hpf) to the indicated Nano-PS and ERSE concentrations, and the survival rates were determined at 96 hpf by light microscopy. Results are presented as scatter plot (n = 6) and mean (black bar). Data were analyzed by Kruskal-Wallis followed by Dunn's posthoc.

Figure S5

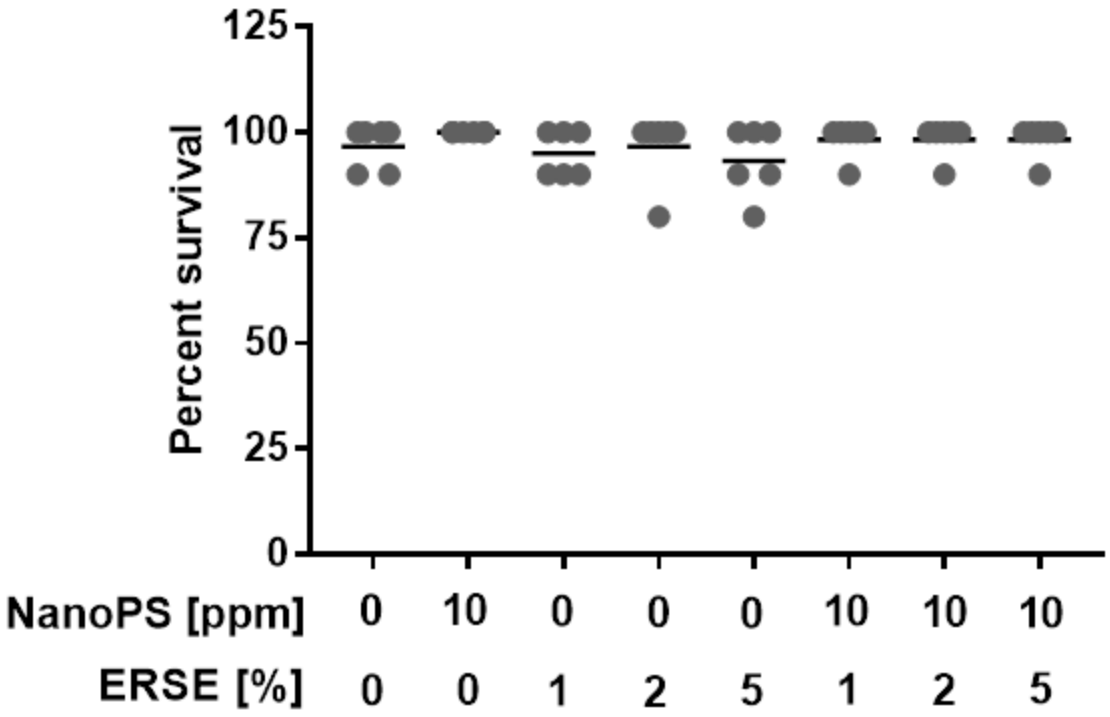

Figure S5: Survival rates of zebrafish larvae exposed to 44 nm nanopolystyrene particles (Nano-PS) in the presence of a real world environmental PAH mixture (Elizabeth River Sediment Extract – ERSE). Embryos were exposed at 6 hours post fertilization (hpf) to the indicated Nano-PS and ERSE concentrations, and the survival rates were determined at 96 hpf by light microscopy. Results are presented as scatter plot (n = 6) and mean (black bar). Data were analyzed by two-way ANOVA followed by Tukey's posthoc.

Figure S6

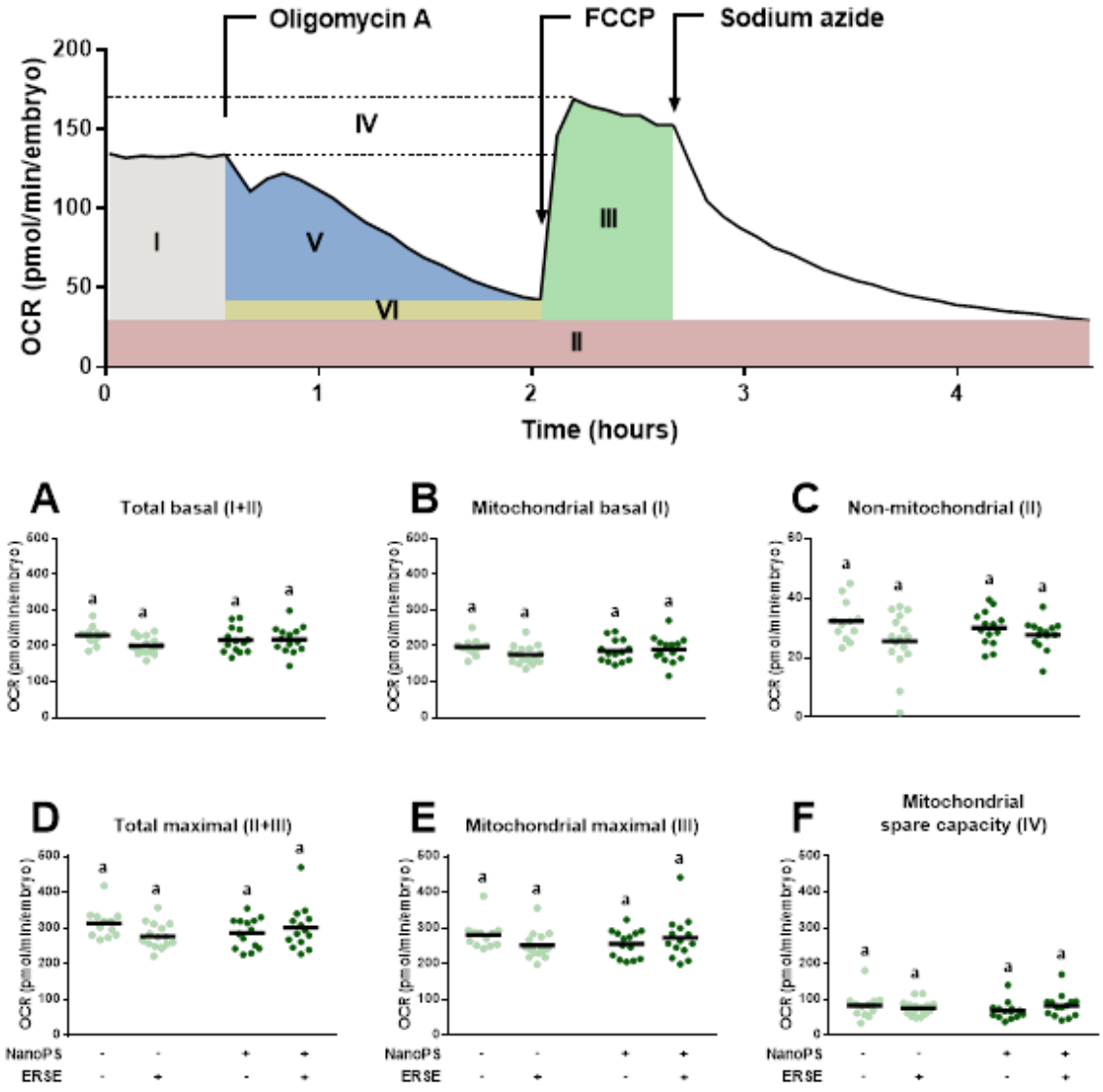

Figure S6: Mitochondrial bioenergetics in zebrafish larvae exposed to 44 nm nanopolystyrene particles (Nano-PS) in the presence of a real world environmental PAH mixture (Elizabeth River Sediment Extract – ERSE). Animals were co-exposed at 6 hours post fertilization (hpf) to 10 ppm Nano-PS and 2% ERSE. Oxygen consumption rate (OCR) was assessed *in vivo* at 96 hpf. The top panel depicts the use of chemical agents to increase mitochondrial OCR to its maximal (FCCP), to completely block it (sodium azide), or to block only the mitochondrial ATP-linked OCR (oligomycin A), and the subsequent division of organismal bioenergetics into different categories (I – VI). Further details are provided in Fig. S1 and the OCR values overtime are shown in Fig. S6. Results are presented as scatter plot (n = 12 – 18) and mean (black bar), and the respective

bioenergetics fraction is shown with a Roman numeral. Data were analyzed by two-way ANOVA followed by Tukey's posthoc. Groups with different letters are significantly different from each other ($p < 0.05$). Please note that the representative image of the OCR measurements indicates the use of oligomycin A, FCCP and sodium azide in a single experiment, but the assays with larvae used only the FCCP + sodium azide combination.

Figure S7

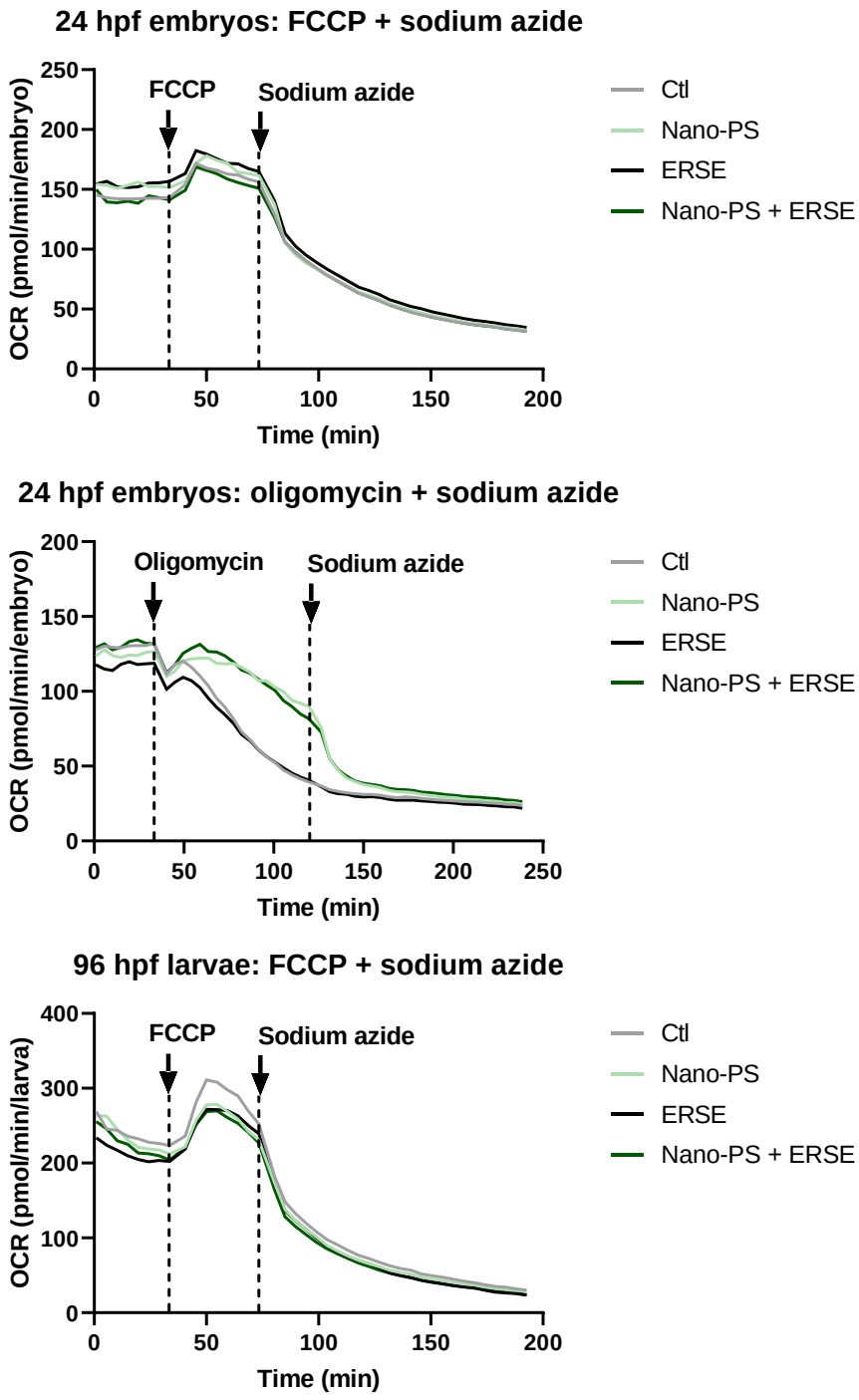

Figure S7: Oxygen consumption rate (OCR) of zebrafish embryos or larvae exposed to 44 nm nanopolystyrene particles (Nano-PS) in the presence of a real world environmental PAH mixture (Elizabeth River Sediment Extract – ERSE). The graphs show the OCR values during the assay,

with the addition of the pharmacological drugs FCCP, oligomycin, and sodium zide to measure the different *in vivo* bioenergetic profiles. Results are presented as average (n = 15 – 24). Please note that the assay is composed of independent runs (FCCP + sodium azide or oligomycin + sodium azide), and larvae were assayed only in the presence of FCCP + sodium azide.

Figure S8

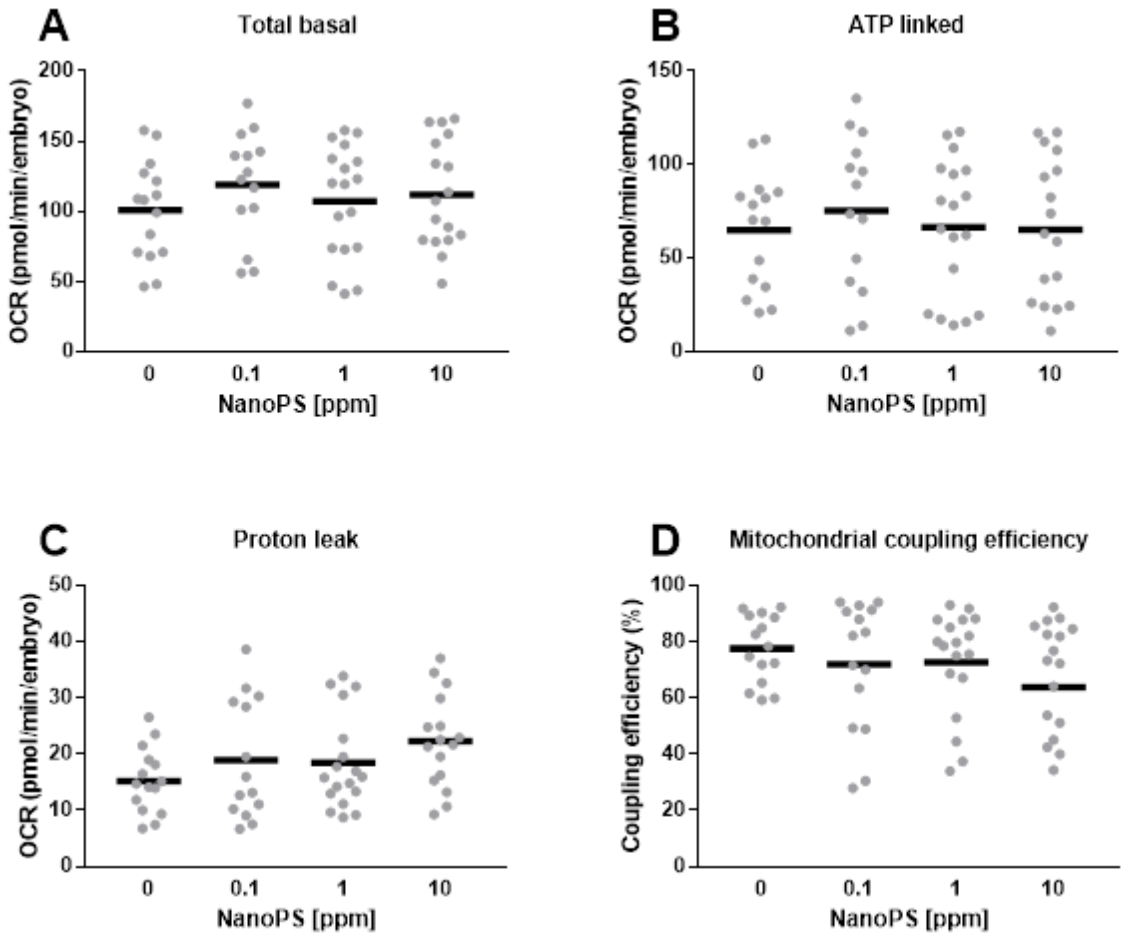

Figure S8: Mitochondrial bioenergetics in zebrafish larvae exposed to 44 nm nanopolystyrene particles (Nano-PS). At 24 hpf, non-exposed embryos were prepared for OCR measurements as usual, except that Nano-PS and oligomycin A were added together to the 24 wells right after the end of basal measurements. In the case that Nano-PS had been able to interact and bind to oligomycin A, the effects of oligomycin A on OCR measurements would be minor and the ATP-linked and proton leak OCRs would be affected. Results are presented as scatter plot (n = 14 – 18) and mean (black bar). Data were analyzed by one-way ANOVA followed by Dunnet's posthoc or Kruskal-Walis followed by Dunn's posthoc. No significant differences were detected.

Figure S9

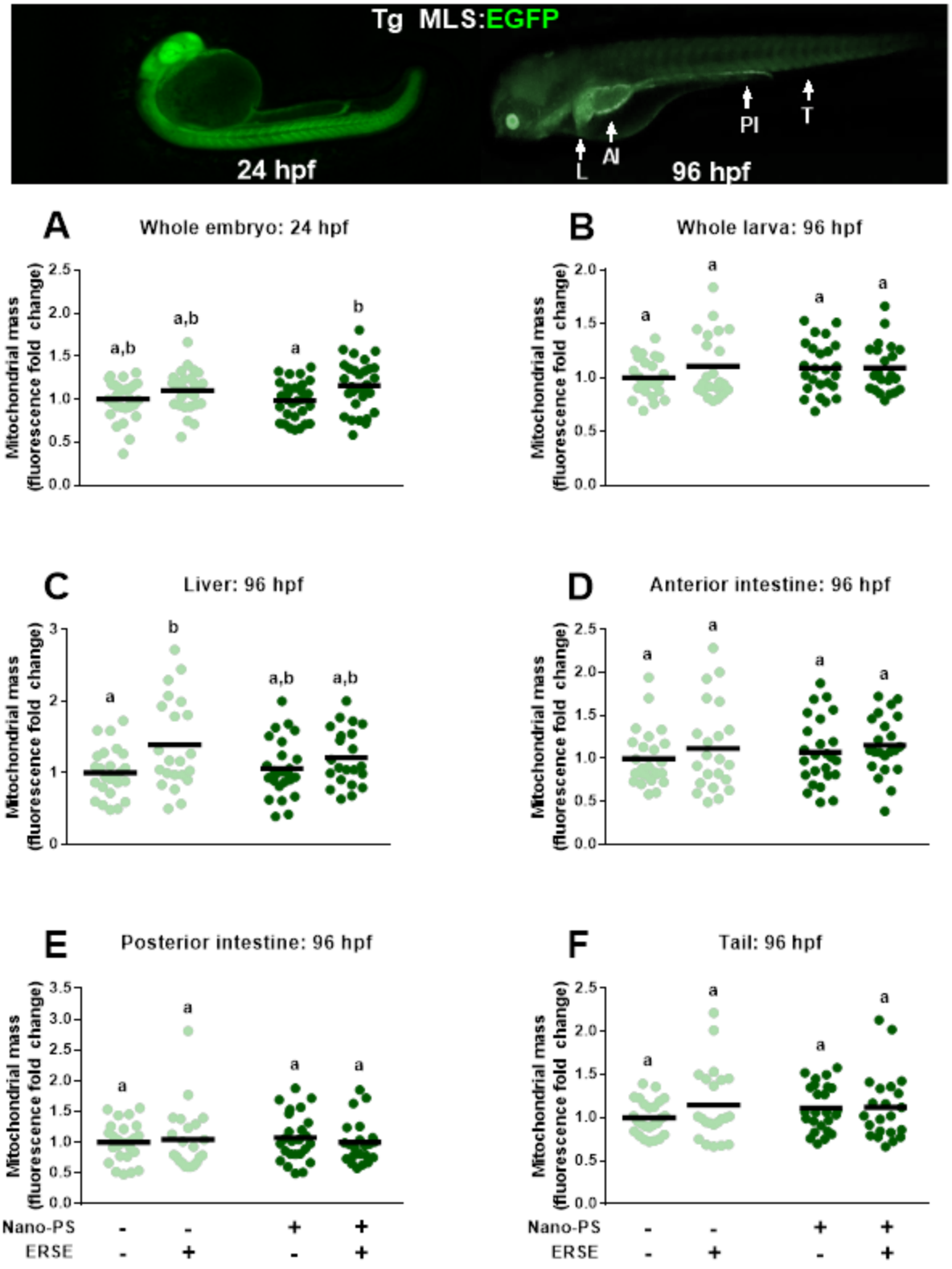
Tg MLS:EGFP
24 hpf
96 hpf
L
AI
PI
T
A
Whole embryo: 24 hpf
B
Whole larva: 96 hpf
C
Liver: 96 hpf
D
Anterior intestine: 96 hpf
E
Posterior intestine: 96 hpf
F
Tail: 96 hpf
Mitochondrial mass (fluorescence fold change)
Nano-PS
ERSE

Figure S9: Mitochondrial mass in zebrafish embryos or larvae exposed to 44 nm nanopolystyrene particles (Nano-PS) in the presence of a real world environmental PAH mixture (Elizabeth River Sediment Extract – ERSE). Animals were co-exposed at 6 hours post fertilization (hpf) to 10 ppm Nano-PS and 2% ERSE, and mitochondrial mass was estimated *in vivo* at 24 or 96 hpf by fluorescence microscopy using the transgenic line Tg (MLS-EGFP). The top panel shows representative images of the transgenic lines at 24 and 96 hpf, as well as the different organs analyzed at 96 hpf: liver (L), anterior intestine (AI), posterior intestine (PI) and tail (T). Results are presented as scatter plot (n = 30) and mean (black bar). Data were analyzed by two-way ANOVA followed by Tukey's posthoc. Groups with different letters are significantly different from each other ($p < 0.05$).